A Novel Fiber-Coated Strong Base-Type Anion Exchanger with Superfast Kinetics. Removal and Recovery of Silver Thiosulfate from Aqueous Solutions

Manas Chanda, S. Arumugom Pillay, Amitava Sarkar, Jayant M. Modak

Department of Chemical Engineering, Indian Institute of Science, Bangalore 560012, India

Received 25 February 2005; accepted 23 August 2005
DOI 10.1002/app.23617
Published online 2 February 2006 in Wiley InterScience (www.interscience.wiley.com).

ABSTRACT: A commercial acrylic fiber with 92% (w/w) acrylonitrile content was partially hydrolyzed converting a fraction of the nitrile (—CN) groups to carboxylic acid (—COOH) groups, to coat the fiber with polyethylenimine (PEI) resin, which was then crosslinked with glutaraldehyde and further quaternized with ethyl chloroacetate to produce a novel strong-base anionic exchanger in the form of fiber. Designated as PAN(QPEI.XG)(Cl^-), the fibrous sorbent was compared with a commercial bead-form resin Amberlite IRA-458(Cl^-) in respect of sorption capacity, selectivity, and kinetics for removal of silver thiosulfate complexes from aqueous solutions. Though the saturation level of $[Ag(S_2O_3)_2]^{3-}$ on PAN(QPEI.XG)(Cl^-) is considerably less than that on IRA-458(Cl^-), the gel-coated fibrous sorbent exhibits, as compared to the bead-form sorbent, a significantly higher sorption selectivity for the silver thiosulfate complex in the presence of excess of other anions such as $S_2O_3^{2-}$, SO_4^{2-}, and Cl^-, and a remarkably faster rate of both sorption and stripping. The initial uptake of the sorbate by the fibrous sorbent is nearly instantaneous, reaching up to ~80% of the saturation capacity within 10 s, as compared to only ~12% on the bead-form sorbent. The high initial rate of uptake fits a shell-core kinetic model for sorption on fiber of cylindrical geometry. With 4*M* HCl, the stripping of the sorbed silver complex from the fibrous sorbent is clean and nearly instantaneous, while, in contrast, a much slower rate of stripping on the bead-form sorbent leads to its fouling due to a slow decomposition of the silver thiosulfate complex in the acidic medium. © 2006 Wiley Periodicals, Inc. J Appl Polym Sci 100: 2604–2613, 2006

Key words: acrylic fiber; anionic exchanger; adsorption; sorbent fabric; silver thiosulfate complex; silver removal and recovery

INTRODUCTION

The discharge of heavy metals with aqueous effluents is both a loss of valuable resources and a source of environmental pollution. The main treatment processes for the removal of metal ions include chemical precipitation, membrane separation, and sorption/ion exchange. Ion exchange sorption is often preferred as it offers the advantages of possible recovery of metal values, minimum space requirement, and recovery of water of sufficient purity for reuse. The subject of metal ion sorption is of major interest at present, as evident from a number of major reviews.[1,2]

Commercial ion-exchange sorbents, commonly supplied in the form of granules or beads, have the drawback that the attainable sorption capacity is often much less than the theoretical capacity due to the inaccessibility of many sorption sites remaining buried inside the bead and this difference becomes greater as the bead/particle size increases. The relative inaccessibility of sorption sites inside the beads also results in relatively slow rates of sorption. The slow kinetics, in addition to relatively high cost of ion-exchange sorbents, is an important factor preventing large scale and widespread applications of the ion-exchange method of separation. Considerable research was therefore directed in recent years at developing ion exchange/chelating sorbents of significantly faster kinetics. Shell functionalization was a common approach adopted by several workers to achieve faster kinetics. In one approach,[3,4] shell-functionalization was achieved by using a reagent system and a particulate resin in which the functionalization rate was faster than the rate of diffusion of the reagent and stopping the reaction when the most readily accessible sites were functionalized.

A simple process of shell-functionalization was developed by Chanda and Rempel[5–10] in which ion-exchange or chelating resins were gel-coated as a thin layer on a solid support, such as silica or polystyrene, using Cu(II) ions as a transient host. The process employed Cu(II) host ions preloaded on a solid substrate, such as silica[5–8] or polystyrene[9] to build a surface

Correspondence to: M. Chanda (chanda@chemeng.iisc.ernet.in).

Contract grant sponsor: Council of Scientific and Industrial Research, New Delhi; contract grant number: 21/0529/02/EMR-II.s

layer of chelating resin, which was then stabilized by reacting with a suitable crosslinking agent before eventually leaching out the host copper ions. The process produced thin, uniform, and firmly adherent layer of the sorbent resin on a solid substrate of any physical shape and geometry. However, only polymers which would readily react with Cu(II) ions and undergo crosslinking reactions with suitable reagents could be used for gel-coating by this process, yielding sorbents of both high capacity and fast kinetics. Thus, a sorbent prepared in this way by gel-coating poly(4-vinyl pyridine)[6] and quaternized poly(4-vinyl pyridine)[6] on silica using 1,4-dibromobutane as the crosslinking agent, showed a significant increase in the rate of sorption and elution, as compared to conventional bead-form resins, in the sorption of uranium and organic sulfonates, respectively, from dilute aqueous solutions. A similar process was later used for gel-coating polyethyleneimine (PEI) and polyacrylic acid on silica using glutaric dialdehyde[7] and diepoxide[8] as crosslinking agents.

For gel-coating on polystyrene, the resin beads were first oxidized partially, creating carboxyl groups to bind the Cu(II) host ions[9] as required for the above process of gel-coating by chelating resins. In a later study,[10] polyacrylonitrile (PAN) crosslinked with divinyl benzene was used as the particulate base resin to make gel-coated sorbents by a similar process, as it would open up exciting possibilities of producing gel-coated sorbent as fiber or woven fabric[11] for a wide variety of applications, since PAN is readily available in these forms.

For coating PAN fiber with polyethyleneimine (PEI), a limited amount of carboxylic acid functionality (as a sodium salt) was created on the fiber surface and Cu(II) was loaded as host ions to help attract PEI onto the fiber surface from solution, followed by insolubilization of the PEI by crosslinking with glutaraldehyde and finally leaching out the Cu(II) host ions from the gel-coated fiber.[11] Subsequently, the process was simplified[12] to enable direct coating of PEI, without Cu(II) mediation, on the partially hydrolyzed PAN fiber (in acid form) followed by insolubilization with glutaraldehyde. The polymeric sorbent thus obtained in fiber form, designated as PAN(CO_2H)(PEI.XG) contains both carboxylic-type cation exchange functionality and secondary/tertiary amine groups to serve as weak-base anion-exchange and chelating sites.

In the present work, the sorbent PAN(CO_2H)(PEI.XG) was converted into strongly basic anion-exchange fibrous sorbent by quaternization with ethyl chloroacetate.[13] The resulting sorbent in fiber form, designated as PAN(QPEI.XG)(Cl^{-1}) exhibited very fast sorption capacity for soluble anionic complexes of heavy metals in water. This is illustrated in the present article with a study made on the sorption and desorption of silver thiosulfate complexes from aqueous solutions.

The presence of soluble silver in waste water is a problem shared by many industries, the two major sources being the photographic and electroplating industries. A large amount of silver is used in photography as fine grains of silver bromide suspended in a thin layer of gelatin forming a photographic emulsion. The undeveloped grains of silver bromide are removed by a fixing solution containing the thiosulfate ion which forms the soluble silver thiosulfate complex. The photographic rinses and effluents thus contain silver thiosulfate complexes in aqueous thiosulfate solutions.

Silver being a valuable metal, a number of recovery methods have had a history of use. For recovery of silver from photographic fixing or (color) bleach-fixing solutions, electrochemical reduction is often used and efficient electrolytic silver recovery units are commercially available. Though 90–98% pure silver can be recovered from cathode, longer operation leads to the formation of silver sulfide sludge. Precipitation and ion-exchange are two additional methods currently employed to remove silver from wastewater. All these methods, however, have associated problems.[14] Electrodeposition is an expensive process and, moreover, it does not remove silver at low concentrations. Replacement by metals is cheaper, but the process removes only about 95% of the silver from the solution, and the treated wastewater can still be above the permissible limit (5 ppm). Both the processes, moreover, produce sludge that is expensive to refine. The precipitation method can reduce the silver concentration to the desired limit but require the use of large amounts of chemicals, producing a large body of sludge to be treated.

In comparison with the above methods, the ion-exchange method is effective even at low silver concentrations. Studies have demonstrated[15] that traces of silver thiosulfate complexes can be recovered using a type-I strong base anion exchange resin in the salt form and eluting the adsorbed silver using 4*M* HCl. The ion-exchange method, however, is relatively expensive. Chitosan,[16] produced from natural polymer chitin, is effective in removing silver ions from water even in low concentrations,[17] but it can remove silver thiosulfate complex only at acidic pH below 4 and does not sorb these complexes in the pH range 4–10. [17] In comparison, a strongly basic, quaternary ammonium functional resin, such as Amberlite IRA-458, is effective[17] in removing silver thiosulfate complexes over the entire pH range 2–10. Since the resin coat of the novel gel-coated sorbent PAN(QPEI.XG)(Cl^-) developed in the present work has quaternary ammonium functional groups, this sorbent was used for studying the sorption of silver thiosulfate complexes from aqueous solutions to take advantage of the superfast kinetic behavior of the fibrous sorbent. For comparison, the corresponding sorption measure-

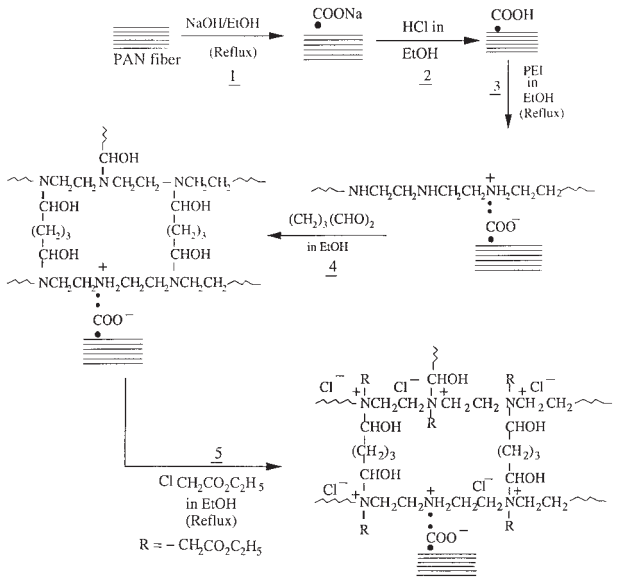

Figure 1 Schematic of the method of preparation of gel-coated fibrous sorbent PAN(QPEI.XG)(Cl^-) by chemically coating and crosslinking polyethylenimine (PEI) on textile-grade polyacrylonitrile (PAN) fiber, followed by quaternization with ethyl chloroacetate.

ments were also performed with strongly basic anion exchange resin Amberlite IRA-458 in chloride form. Both equilibrium sorptions and sorption kinetics were measured to explore the benefits of using gel-coated fibrous sorbent as compared to the conventional bead-form sorbent.

EXPERIMENTAL

Materials

A commercial branched polyetheylenimine (PEI) (Aldrich Cat. No. 18,197–8) of average molecular weight 60,000 was used for gel-coating of acrylic fiber. Textile grade acrylic fiber, *Cashmilon*™, of composition (by wt.) acrylonitrile 92%, methyl acrylate 6%, and sodium methallyl sulfonate 2%, used in the work, was obtained from Indian Petrochemical Corp. Ltd., Baroda, Gujarat, India. (Henceforth the acrylic fiber will be referred to simply as PAN fiber.) Amberlite IRA-458 (strongly basic, quaternary ammonium functional group, capacity 4.6 meq/g) was obtained from Sigma Chemical Co., St. Louis, MO. It was used in chloride form as supplied and was only given a thorough wash with water before use.

Sorbent

The method of gel-coating the PAN fiber with PEI and converting it into quaternary ammonium type sorbent is shown schematically in Figure 1. PAN was partially converted to —CO_2Na by reacting with 10% (w/v) solution of NaOH in ethanol under reflux for 20 h (Step 1) and then washed with ethanol to remove free alkali. The product was designated as PAN(CO_2Na). In Step 2, PAN(CO_2Na) was treated with dilute solution of HCl in ethanol to convert the partially hydrolyzed fiber into the free-acid (—COOH) form, which was then added to 5% (w/v) PEI resin solution in ethanol and refluxed for 10 h (Step 3). The resulting PEI-coated fiber was washed with ethanol to remove any free resin and treated with 5% (w/v) solution of glutaraldehyde in ethanol for 10 h for crosslinking, i.e., gel formation and insolubilization of PEI (Step 4). The product, designated as PAN(PEI.XG) was quaternized by heating in 30% (v/v) solution of ethyl chloroacetate in ethanol under reflux for 10 h, washed free of this reagent with ethanol, and then dried in oven at 70°C. The resulting fibrous sorbent containing gel-coated ammonium resin in chloride form was designated as PAN(QPEI.XG)(Cl^-).

The proton capacity of the precursor sorbent PAN-(PEI.XG), measured in 0.10*N* HCl, is 3.4 meq/g (dry), while that of PEI.XG prepared separately by reacting (crosslinking) PEI with glutaraldehyde under identical conditions is 11.7 meq/g, indicating that the extent of resin coating in PAN(PEI.XG) is about 29% by weight.

The elemental compositions of PAN(QPEI.XG)(Cl^-) and its precursors are recorded in Table I. The precursor PAN(PEI.XG) shows an increase in oxygen content, compared to that of PAN(CO_2H), due to the coating of PEI.XG, while its IR spectrum, shown in Figure 2 confirms the presence of amine groups. The elemental composition of PAN(QPEI.XG)(Cl^-) shows further increase in oxygen and presence of Cl due to quaternization with ethyl chloroacetate ($C_4H_7O_2Cl$), while the IR spectrum shows the presence of quaternary ammonium functional group. The properties of PAN(QPEI.XG)(Cl^-) sorbent (dry) are presented in Table II.

The resin gel-coat on the fiber is found to have remarkably good adhesion and stability to repeated cycles of sorption and regeneration. This may be attributed to three factors: (a) the coating takes place via reaction of the polyimine from the solution with surface carboxyl groups; (b) the polyimine chains on the fiber surface are highly crosslinked; (c) as the PAN

TABLE I
Comparison of Elemental Compositions of Gel-Coated Fibrous Sorbent PAN(QPEI.XG)(Cl^-) and its Precursors

Sample	Elemental composition, % (w/w)				
	C	H	N	O	Cl
PAN	66.1	5.8	23.7	2.1	—
PAN(CO_2H)	64.5	6.7	21.3	8.6	—
PAN(PEI.XG)	62.1	6.7	20.2	11.4	—
PAN(QPEI.XG)(Cl^-)	56.4	6.4	14.8	15.0	7.4

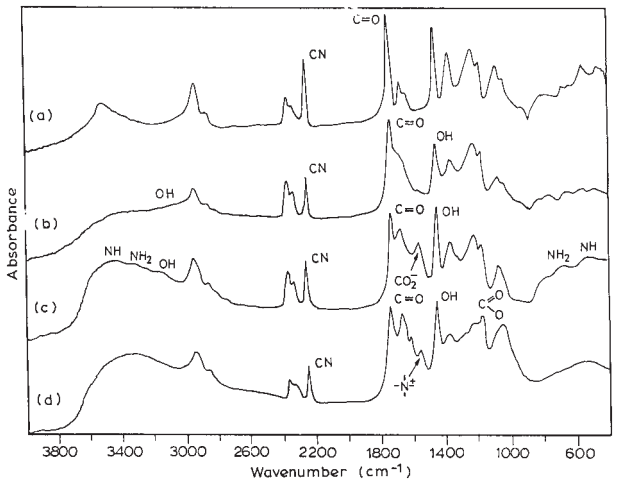

Figure 2 Comparison of FTIR spectra of (a) polyacrylonitrile fiber (*Cashmilon*™), (b) partially hydrolyzed fiber PAN(CO_2H), (c) gel-coated fiber PAN(PEI.XG), and (d) quaternized gel-coated fiber PAN(QPEI.XG)(Cl^-)

fiber is made by the wet spinning process, it has extremely rough surface with longitudinal serrations, which facilitate strong adherence of the coated resin to the fiber surface.

Analysis

The concentration of Ag in aqueous thiosulfate solutions was measured by atomic absorption spectrometry, while thiosulfate was estimated by iodimetry.[18] The well-known Volhard's method[18] was used for Cl^- estimation.

Sorbate

A variety of silver thiosulfate salts have been reported in the literature, but it is generally agreed that only four of these are stable under ordinary conditions.[19] Though it has been reported[19] that $[Ag(S_2O_3)_2]^{3-}$ is the predominant species in solution and that no species richer in silver than $[Ag(S_2O_3)_2]^{3-}$ exists in solution, it is apparent that the number and stoichiometry of the silver/thiosulfate complex species existing in solution is uncertain and the relative concentrations of Ag^+ and $S_2O_3^{2-}$ are key factors controlling the complexation phenomena. For sorption studies in the present work, aqueous solutions of $Na_3Ag(S_2O_3)_2$ were made by stirring pure AgCl (99.99%) in a solution of sodium thiosulfate (99.5%) in purified water with AgCl: $Na_2S_2O_3$ mole ratio of 1 : 2, which resulted in dissolution of 96% of AgCl. The solution was filtered and the concentration of Ag determined by Atomic Absorption Spectrophotometry. Since the average mole ratio of Ag and $S_2O_3^{2-}$ in the solution was very nearly 1:2 and $[Ag(S_2O_3)_2]^{3-}$ is known as the ion of maximum stability, this will be considered as the sole sorbate species for simplicity of calculations. For all the experimental work, purified water, prepared by treating boiled-out distilled water with a mixture of Amberlite IR-120 and Amberlite IRA-400 ion-exchange resins and stored under nitrogen, was used. The solution of silver thiosulfate made above with $Ag^+/S_2O_3^{2-}$ mole ratio 1:2 and stored under N_2 in the dark was stable over several weeks.

Sorption experiments

Sorption measurements were made separately with PAN(QPEI.XG)(Cl^-) and IRA-458(Cl^-) using $Ag/S_2O_3^{2-}$ (1 : 2) complex as the test sorbate. For equilibrium sorption measurements, small scale dynamic contact between the sorbent fibers cut into small pieces and the sorbent solution of specified composition was effected for 10 h (since the sorption rate slows down abruptly after the initial very high rate) in tightly stoppered flasks at 30°C on a mechanical shaker kept in a dark chamber. The extent of sorption was calculated from the residual concentration of the sorbate in the equilibrated solution. A range of concentrations of the sorbate were used.

For the measurement of sorption kinetics, PAN(QPEI.XG)(Cl^-) fiber, cut into 3 cm long strands and pre-soaked in water for 1 h, was used. A rectangular basket (20 mm ×15 mm ×50 mm) made of polypropylene mesh (0.60 mm opening) was used to hold the sorbent. The basket was fitted to the shaft of a motor and rotated while the sorbate solution was brought to it and held for a specified period. This allowed the sorbent to be instantly separated from the sorbate solution at any desired time and the residual concentration of the sorbate measured to determine the rate of sorption. A fresh amount of the sorbent from the same stock was used for each experiment. For the purpose of comparison, the sorption rates were also measured under the same conditions using the commercial resin Amberlite IRA-458(Cl^-) in spherical bead form.

Initially the sorption rates were measured at different stirring speeds using a low solution concentration (2.0 mmol/L) to determine the minimum speed above

TABLE II
Properties of Gel-Coated Sorbent Fiber PAN(QPEI.XG)(Cl^-) Used for Sorption of Silver Thiosulfate Complex

Water content	4% (w/w)
Fiber diameter (average)	20 μm
Fiber length	3 cm
BET surface area	1.1 m^2/g dry
Pore volume	0.53 cm^3/g dry
Exchange capacity	2.50 meq/g dry

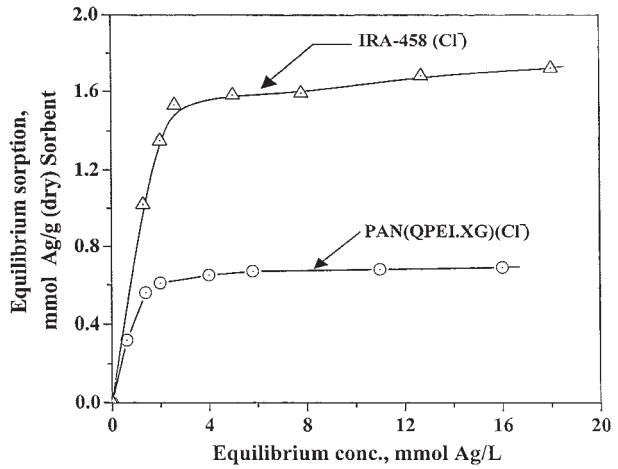

Figure 3 Equilibrium sorption isotherms for $[Ag(S_2O_3)_2]^{3-}$ on PAN(QPEI.XG)(Cl^-) and IRA-458(Cl^-). Sorbent loading: PAN(QPEI.XG)(Cl^-) 6 g (dry)/L, IRA-458(Cl^-) 1.6 g (dry)/L; pH 5; temperature 30°C.

which the sorption rate was not influenced by the degree of agitation and hence not controlled by film diffusion. All kinetic measurements were performed using stirring speeds well above the minimum.

RESULTS AND DISCUSSION

Sorption isotherm

The equilibrium sorption data of $[Ag(S_2O_3)_2]^{3-}$ on PAN(QPEI.XG)(Cl^-) and IRA-458(Cl^-) are presented graphically in Figure 3. For the sorbate species $[Ag(S_2O_3)_2]^{3-}$, the sorption on PAN(QPEI.XG)(Cl^-) takes place by the anion-exchange reaction

$$\rightarrow N^+RCl^- + [Ag(S_2O_3)_2]^{3-} \rightarrow\rightarrow$$
$$N^+R\cdots[Ag(S_2O_3)_2]^{3-}/3 + Cl^- \quad (1)$$

Similar anion exchange sorption also takes place on IRA-458(Cl^-) which, however, shows considerably higher sorption due to its higher capacity.

The sorption data on both the sorbents fitted well to both the Langmuir and Freundlich isotherms, though the former gave a somewhat better fit. Defining the parameters A_s and K_b as the saturation sorption capacity (mmol Ag/g dry sorbent) and the sorption binding constant (L/mol), respectively, the Langmuir isotherm is written as

$$\chi^* = \frac{(10^{-3}K_b)A_sC^*}{1 + (10^{-3}K_b)C^*} \quad (2)$$

where x^* is the equilibrium sorption (mmol Ag/g dry sorbent) and C^* is the equilibrium sorbate concentration (mmol Ag/L) in the solution.

The Freundlich isotherm is written as

$$\chi^* = p(C^*)^{1/q} \quad (3)$$

where p and q are parameters, and x^* and c^* are as defined above.

The values of the parameters A_s, K_b, p, and q for $[Ag(S_2O_3)_2]^{3-}$ sorption determined by least squares fit of the sorption data in Figure 3 are presented in Table III. The same parameters evaluated from the $S_2O_3^{2-}$ and SO_4^{2-} sorption data (Figs. 4 and 5) on PAN(QPEI.XG)(Cl^-) and IRA-458(Cl^-) are also recorded in Table III.

TABLE III
Langmuir and Freundlich Isotherm Parameters for Sorption of $[Ag(S_2O_3)_2]^{3-}$ on PAN(QPEI.XG)(Cl^-)

Sorbate/sorbent	Langmuir isotherm, eq. (2) A_s (mmol/g dry sorbent)	k_b (L/mol)	Corr. coeff.
$Ag(S_2O_3)_2^{3-}$/PAN(QPEI.XG)(Cl^-)	0.759	1568	0.998
$Ag(S_2O_3)_2^{3-}$/IRA-458(Cl^-)	1.852	1078	0.996
$S_2O_3^{2-}$/PAN(QFEI.XG)(Cl^-)	1.16	129	0.996
$S_2O_3^{2-}$/IRA-458(Cl^-)	2.038	1254	0.995
SO_4^{2-}/PAN(QPEI.XG(Cl^-)	0.705	187	0.999
SO_4^{2-}/IRA-458(Cl^-)	1.821	908	0.999

Sorbate/sorbent	Freundlich isotherm, eq. (3) p	q	Corr. coeff.
$Ag(S_2O_3)_2^{3-}$/PAN(QPEI.XG)(Cl^-)	0.418	3.424	0.844
$Ag(S_2O_3)_2^{3-}$/IRA-458(Cl^-)	0.868	2.595	0.903
$S_2O_3^{2-}$/PAN(QPEI.XG)(Cl^-)	0.145	1.468	0.997
$S_2O_3^{2-}$/IRA-458(Cl^-)	0.993	2.665	0.993
SO_4^{2-}/PAN(QPEI.XG)(Cl^-)	0.121	1.613	0.990
SO_4^{2-}/PAN-458(Cl^-)	0.958	3.884	0.977

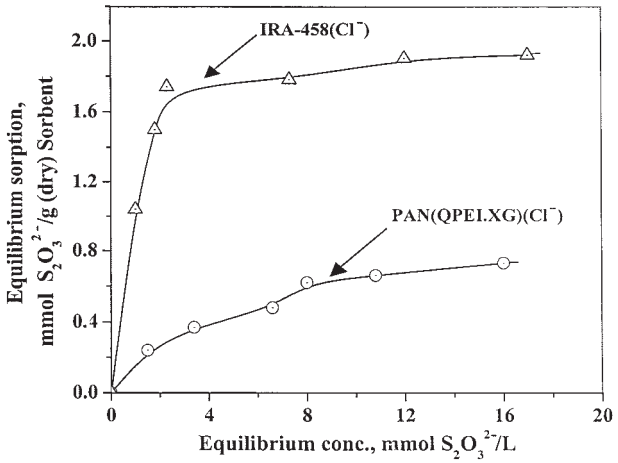

Figure 4 Equilibrium sorption isotherms for $S_2O_3^{2-}$ on PAN(QPEI.XG)(Cl^-) and IRA-458(Cl^-). Sorbent loading: PAN(QPEI.XG)(Cl^-) 6 g (dry)/L, IRA-458(Cl^-) 1.6 g (dry)/L; pH 5; temperature 30°C.

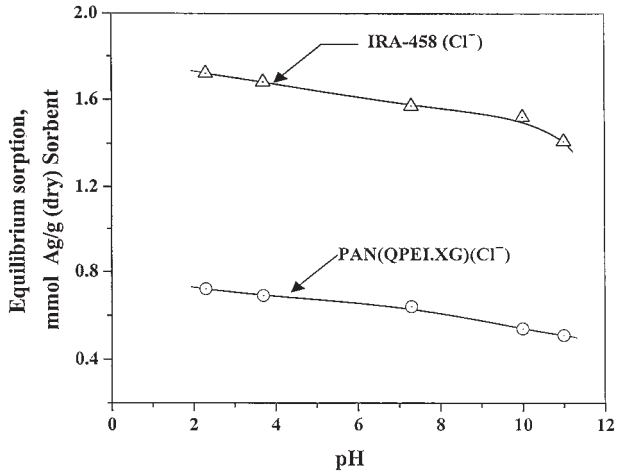

Figure 6 Effect of pH on sorption of $[Ag(S_2O_3)_2]^{3-}$ on PAN(QPEI.XG)(Cl^-) and IRA-458(Cl^-). Sorbent loading: PAN(QPEI.XG)(Cl^-) 6 g (dry)/L, IRA-458(Cl^-) 1.6 g (dry)/L; temperature 30°C.

A comparison of A_s and K_b values for $[Ag(S_2O_3)_2]^{3-}$ shows that while IRA-458(Cl^-) has higher saturation sorption capacity than PAN(QPEI.XG)(Cl^-), the latter has higher binding constant, which may have a significant bearing on the sorption selectivity for $[Ag(S_2O_3)_2]^{3-}$ in the presence of other anions such as $S_2O_3^{2-}$ and SO_4^{2-}, since for both the latter species, IRA-458(Cl^-) has much higher sorption capacity but much lower binding constant than that of PAN(QPEI.XG)(Cl^-).

Effect of pH

To determine the effect of pH on the sorption of silver/thiosulfate complexes, the pH of the solution concentration was adjusted in the acidic range with glacial acetic acid and in the alkaline range with ammonia solution, respectively. The sorption data on PAN(QPEI.XG)(Cl^-) and IRA-458(Cl^-), plotted in Figure 6, show that on both the sorbents the sorption is not affected in moderately acidic solution, while in alkaline media the sorbents remain active even at relatively high pH. This is important since photographic fixing solutions are alkaline and have relatively high thiosulfate content for stability.

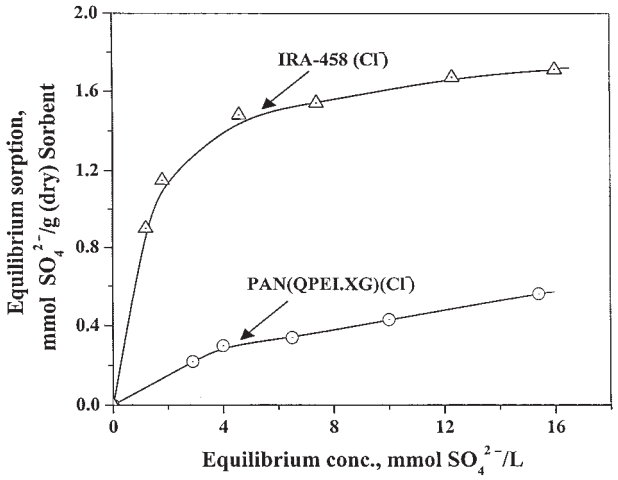

Figure 5 Equilibrium sorption isotherms for SO_4^{2-} on PAN(QPEI.XG)(Cl^-) and IRA- 458(Cl^-). Sorbent loading: PAN(QPEI.XG)(Cl^-) 6 g (dry)/L, IRA-458(Cl^-) 1.6 g (dry)/L; pH 5; temperature 30°C.

Effect of common anions

The equilibrium sorptions of $[Ag(S_2O_3)_2]^{3-}$ on PAN(QPEI.XG)(Cl^-) and IRA-458(Cl^-) in the presence of varying concentrations of Na_2SO_4 and NaCl are plotted in Figures 7 and 8, respectively. It is seen that even at high concentrations, Na_2SO_4 has no effect on the Ag sorption capacity of the gel-coated sorbent, while the capacity of IRA-458(Cl^-) is markedly reduced by Na_2SO_4. Interestingly, the chloride ion is seen to exert a stronger stripping effect on both the sorbents. The effect, however, is significantly more pronounced on IRA-458(Cl^-), so much so that in strong NaCl (>12% w/v) solution, its Ag sorption capacity is even less than that of PAN(QPEI.XG)(Cl^-).

Binary sorption isotherm

The equilibrium sorption data on PAN(QPEI.XG)(Cl^-) and IRA-458(Cl^-) in binary sorption systems $[Ag(S_2O_3)_2]^{3-}/S_2O_3^{2-}$ and $[Ag(S_2O_3)_2]^{3-}/SO_4^{2-}$ are compared in Figures 9 and 10. The data show that the PAN(QPEI.XG)(Cl^-) sorbent removes $[Ag(S_2O_3)_2]^{3-}$ trivalent ions in preference to both $S_2O_3^{2-}$ and SO_4^{2-}

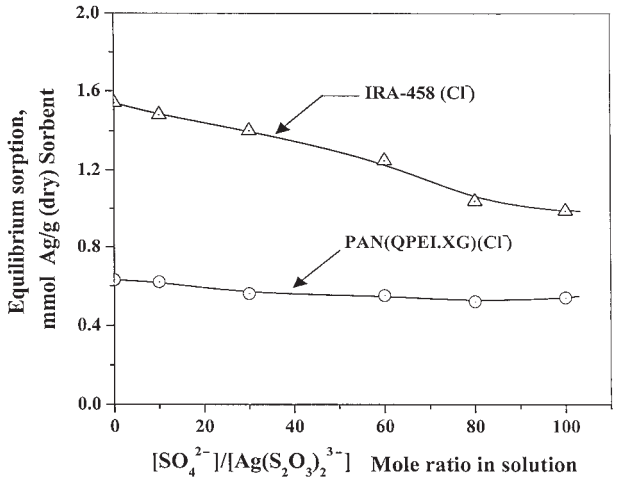

Figure 7 Effect of Na_2SO_4 on sorption of $[Ag(S_2O_3)_2]^{3-}$ on PAN(QPEI.XG)(Cl^-) and IRA-458(Cl^-). Sorbent loading: PAN(QPEI.XG)(Cl^-) 6 g (dry)/L, IRA-458(Cl^-) 1.6 g (dry)/L; initial concentration of $[Ag(S_2O_3)_2]^{3-}$ in solution 10 m*M*; pH 5; temperature 30°C.

and, in this respect, it is superior to the commercial sorbent IRA-458(Cl^-).

Several models are available for predicting adsorption from multicomponent solutions of species obeying the pure component equations. For binary sorption, the Butler–Ockrent model[20] can be written as

$$\chi_i^* = \frac{A_{s,i}K_{b,i}C_i}{1 + K_{b,1}C_1 + K_{b,2}C_2} (i = 1 \text{ or } 2) \qquad (4)$$

If there is a competition for all available sites, this Langmuir-like model may satisfactorily predict the extent of sorption from a binary system.[21] However, if

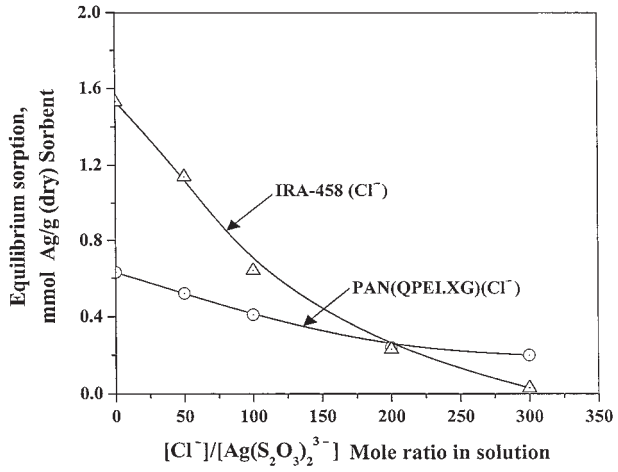

Figure 8 Effect of NaCl on sorption of $[Ag(S_2O_3)_2]^{3-}$ on PAN(QPEI.XG)(Cl^-) and IRA-458(Cl^-). Sorbent loading: PAN(QPEI.XG)(Cl^-) 6 g (dry)/L, IRA-458(Cl^-) 1.6 g(dry)/L; initial concentration of $[Ag(S_2O_3)_2]^{3-}$ in solution 10 m*M*; pH 5; temperature 30°C.

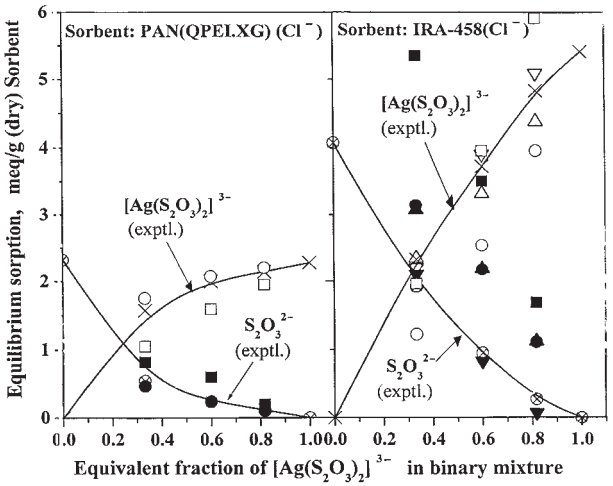

Figure 9 Comparison of experimental sorption values of $[Ag(S_2O_3)_2]^{3-}$ and $S_2O_3^{2-}$ with those calculated from different bicomponent sorption models for different compositions of the bicomponent solution. Sorbent loading: PAN(QPEI.XG)(Cl^-) 30 g (dry)/L; IRA-458(Cl^-) 8 g (dry)/L. Total concentration of $[Ag(S_2O_3)_2]^{3-}$ and $S_2O_3^{2-}$ in solution initially: 0.10 mol/L; feed solution pH 6.0; temperature 30°C. [⊗, 196 ; : experimental; ○, ●: Butler–Ockrent; △, ▲: Jain–Snoeyink; ▽, ▼: LeVan–Vermeulen (Langmuir); □, ■: LeVan–Vermeulen (Freundlich)].

the sorption of either component of a binary system occurs on sites that are inaccessible to one of the species, the Langmuir-like model for competitive sorption is not expected to yield accurate results.

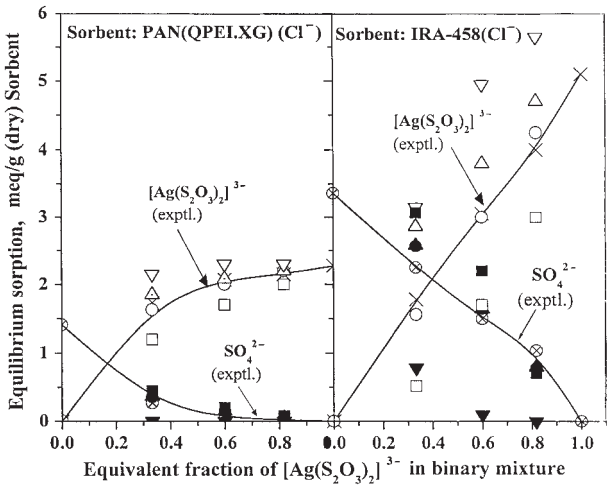

Figure 10 Comparison of experimental sorption values of $[Ag(S_2O_3)_2]^{3-}$ and SO_4^{2-} with those calculated from different bicomponent sorption models for different compositions of the bicomponent solution. Sorbent loading: PAN(QPEI.XG)(Cl^-) 30 g (dry)/L; IRA-458(Cl^-) 8 g (dry)/L. Total concentration of $[Ag(S_2O_3)_2]^{3-}$ and SO_4^{2-} in solution initially: 0.10 mol/L; feed solution pH 6.0; temperature 30°C. [⊗, 196 : experimental; ○, ●: Butler–Ockrent; △, ▲: Jain–Snoeyink; ▽, ▼: LeVan–Vermeulen (Langmuir); □, □: LeVan–Vermeulen (Freundlich)].

The Butler–Ockrent model for binary sorption was modified by Jain and Snoeyink,[21] based on the hypothesis that sorption without competition occurs on some sites when the capacities are not equal and that the number of sites for noncompetitive sorption is proportional to the difference between the maximum loadings of the species, i.e., $(A_{s,1}–A_{s,2})$, where $A_{s,1} > A_{s,2}$. On this basis, the following equations were described:

$$\chi_1^* = \frac{(A_{s,1} - A_{s,2})K_{b,1}C_1^*}{1 + K_{b,1}C_1^*} + \frac{A_{s,2}K_{b,1}C_1^*}{1 + K_{b,1}C_1^* + K_{b,2}C_2^*} \quad (5)$$

$$\chi_2^* = \frac{A_{s,2}K_{b,2}C_2^*}{1 + K_{b,1}C_1^* + K_{b,2}C_2^*} \quad (6)$$

The first term on the right side of eq. (5) is the Langmuir-like expression for the amount of component 1 that sorbs without competition, while the second term, based on the Langmuir-like model for competitive sorption, represents the amount of component 1 sorbed on the surface in competition with component 2.

For $A_{s,2} > A_{s,1}$, the binary component equations take the form:

$$\chi_1^* = \frac{A_{s,1}K_{b,1}C_1^*}{1 + K_{b,1}C_1^* + K_{b,2}C_2^*} \quad (7)$$

$$\chi_2^* = \frac{(A_{s,2} - A_{s,1})K_{b,2}C_2^*}{1 + K_{b,2}C_2^*} + \frac{A_{s,1}K_{b,2}C_2^*}{1 + K_{b,1}C_1^* + K_{b,2}C_2^*} \quad (8)$$

It may be noted that for $A_{s,1} = A_{s,2}$, eqs. (5)–(8) reduce to eq. (4) of the Butler–Ockrent model.

When the capacities of the two components in a bicomponent system are different, the LeVan–Vermeulen model can be represented by a Taylor series that converges very rapidly and can be limited in most cases to its first two or three terms. The second-order Taylor series approximation of the isotherm for component 1 can be written[22] as

$$\chi_1^* = \frac{\bar{A}_s K_1^*}{1 + K_1^* + K_2^*} + \Delta_{L2} \quad (9)$$

where $K_1^* = K_{b,1}C_1^*, K_2^* = K_{b,2}C_2^*$, and $\bar{A}_s$ is a weighted saturation capacity, given by

$$\bar{A}_s = \frac{A_{s,1}K_1^* + A_{s,2}K_2^*}{K_1^* + K_2^*} + 2\frac{(A_{s,1} - A_{s,2})^2}{A_{s,1} + A_{s,2}} \frac{K_1^*K_2^*}{(K_1^* + K_2^*)^2}\left[\left(\frac{1}{K_1^* + K_2^*} + \frac{1}{2}\right) \times \ln(1 + K_1^* + K_2^*) - 1\right] \quad (10)$$

Furthermore,

$$\Delta_{L2} = (A_{s,1} - A_{s,2})\frac{K_1^*K_2^*}{(K_1^* + K_2^*)^2} \ln(1 + K_1^* + K_2^*) \quad (11)$$

The isotherm for component 2 can be obtained by interchanging the component subscripts.

A two-term binary Freundlich isotherm[22] can be similarly derived using LeVan–Vermeulen procedure, yielding

$$x_1^* = \frac{\bar{n}P_1^*}{(P_1^* + P_2^*)^{1-\bar{n}}} + \Delta_{F2} \quad (12)$$

where $P_1^* = C_1^*(p_1/n_1)^{1/n_1}$, $P_2^* = C_2^*(p_2/n_2)^{1/n_2}$ and $\bar{n}$ is a weighted exponent given by

$$\bar{n} = \frac{n_1P_1^* + n_2P_2^*}{P_1^* + P_2^*} \quad (13)$$

Furthermore,

$$\Delta_{F2} = (n_1 - n_2)\frac{P_1^*P_2^*}{(P_1^* + P_2^*)^{2-\bar{n}}} \ln(P_1^* + P_2^*) \quad (14)$$

As before, the isotherm for component 2 can be obtained by interchanging component subscripts. The parameters p_1 and n_1 $(= 1/q_1)$ are the Freundlich parameters of the single-component isotherm for $[Ag(S_2O_3)_2]^{3-}$ and similarly p_2 and n_2 $(= 1/q_2)$ are those for the second component.

By using the single component parameter values as given in Table II, the sorptions of $[Ag(S_2O_3)_2]^{3-}$, $S_2O_3^{2-}$ and SO_4^{2-} from binary mixtures were computed using the four models presented above. These are plotted in Figures 9 and 10 for comparison with experimentally observed values. For the $[Ag(S_2O_3)_2]^{3-}/S_2O_3^{2-}$ binary system, the Butler-Ockrent model is seen to provide a better fit than the other models on PAN(QPEI.XG)(Cl^-) while on IRA-458(Cl^-) only the LeVan–Vermeulen model is seen to give good agreement with experimental data, For the $[Ag(S_2O_3)_2]^{3-}/SO_4^{2-}$ system, however, the Butler–Ockrent model fits the sorption data well on both the sorbents.

Sorption kinetics

The fractional attainment of equilibrium sorption of $[Ag(S_2O_3)_2]^{3-}$ on the fibrous sorbent PAN(QPEI.XG)(Cl^-) and bead-form sorbent IRA-458(Cl^-) was measured as a function of contact time under identical conditions using a rotational speed (200–300 rpm) of the sorbent basket much above the experimentally determined minimum for the elimination of film diffusional resistance. The data plotted in Figure 11 show that the major part of sorption on the gel-coated fiber takes place almost in-

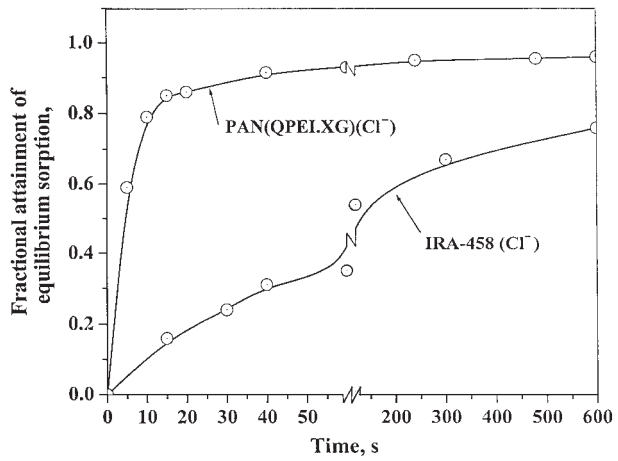

Figure 11 Comparison of rate of sorption of $[Ag(S_2O_3)_2]^{3-}$ on PAN(QPEI.XG)(Cl^-) and IRA-458(Cl^-). Sorbent loading: PAN(QPEI.XG)(Cl^-) 6 g (dry)/L, IRA-458(Cl^-) 1.6 g (dry)/L; pH 5; temperature 30°C; initial sorbate feed concentration 10 m*M*; pH 5; temperature 30°C.

stantaneously, in sharp contrast with the bead-form sorbent on which the sorption takes place slowly over a long period of time. For example, at 10 mM sorbate concentration, about 80% of the equilibrium sorption on the fibrous sorbent is attained in 10 s, while in the same period only 12% of the equilibrium sorption is attained on the bead-form sorbent.

Sorption can be assumed to follow a shell-core scheme if the reaction is irreversible and is fast compared to diffusion. For systems which exhibit significant reversibility in the sorption isotherm, Bhandari et al.[23] modified the shrinking core model by incorporating the effect of the reversibility of sorption. The modified model, however, reduces to the conventional shell-core model as the equilibrium sorption reaches the saturation capacity. In the present study, the sorption isotherm (Fig. 3) of $[Ag(S_2O_3)_2]^{3-}$ on PAN(QPEI.XG)(Cl^-) clearly indicates that the sorption tends to attain the saturation level at sorbate concentrations greater than 4 m*M*. Thus at the feed concentration (10 m*M*) used in the kinetic study, the reversibility of sorption may be ignored and the conventional form of shell-core model based on irreversibility of the sorption reaction may be used. Such a model was derived by Chanda and Rempel[11] for a cylindrical sorbent of very large length/diameter ratio, representing a fiber-like sorbent. The rate of sorption derived from the model is given by the equation:

$$\left(\frac{D\lambda C_0}{r_0^2 \bar{C}_r}\right)t = \frac{\ln\beta}{2\alpha}\ln\left(\frac{\beta^2 + R^{*2}}{\beta^2 + 1}\right) + \sum_{n=1,2\cdots}\frac{\beta^{2n}}{4\alpha n^2}\left\{\frac{1}{(\beta^2 + R^{*2})^n} - \frac{1}{(\beta^2 + 1)^n}\right\} \quad (15)$$

where D = resin diffusivity, λ = molar distribution coefficient, C_o = initial sorbate concentration in solution, $\bar{C}_r$ = sorption capacity per unit volume of unreacted sorbent, r_o = radius of cylindrical sorbent, R^* = radial position (dimensionless) of moving boundary, α = ratio (dimensionless) of sorption on resin at saturation and total amount of sorbate initially in substrate, and

$$\beta = \left(\frac{1 - \alpha}{\alpha}\right)^{1/2} \quad (16)$$

To test the model with experimental sorption data, eq. (15) can be written in terms of fractional conversion $\bar{X}$ by noting that

$$R^* = (1 - \bar{X})^{1/2} \quad (17)$$

Equation (15) combined with eq. (17) gives the sorbent conversion as a function of time. The right hand side (RHS) of eq. (15) can thus be plotted against t and λD can be evaluated from the slope of the linear plot. The sorbent conversion data from Figure 11 are plotted in Figure 12, which shows an approximately linear fit in the initial region extending from 0 to ~80% conversion of the fibrous sorbent, followed by a sharp deviation. This reflects the fact that, as can be seen from Figure 11, beyond about 80% conversion, the rate of sorption slows down abruptly, which may be attributed to several factors, the more important among them being the possible decrease in the reacted layer diffusivity with conversion.

From the slope of the linear plot in the initial region (Fig. 12), λD was calculated, yielding a value of 7.6 $\times$ 10^{-6} cm^2/s corresponding to the initial sorbate concentration of 10 m*M* used in the experiment. The markedly high initial rate of sorption on the gel-coated fiber is attributed to a high percentage of surface area

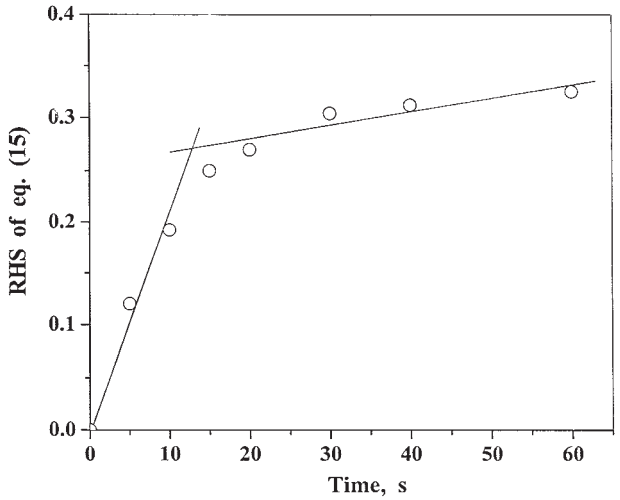

Figure 12 Test of eq. (15) with data of Figure 11 for sorption of $[Ag(S_2O_3)_2]^{3-}$ on PAN(QPEI.XG)(Cl^-).

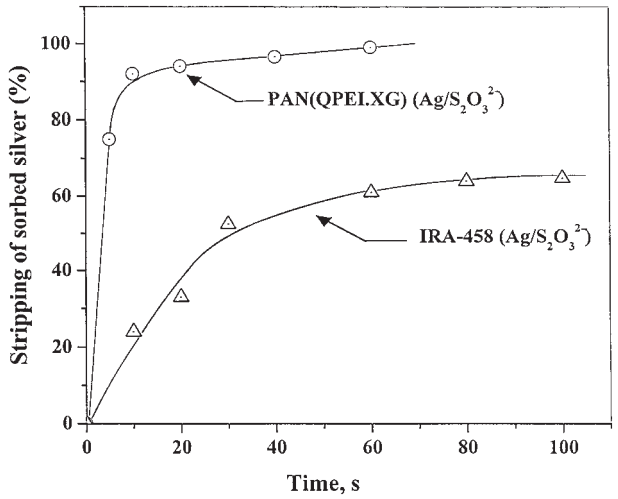

Figure 13 Comparison of rate of stripping of $[Ag(S_2O_3)_2]^{3-}$ on PAN(QPEI.XG)(Cl^-) and IRA-458(Cl^-) with 4*M* HCl at 30°C. Initial silver loading: 0.7 mmol/g (dry) on PAN(QPEI.XG)(Cl^-), and 1.2 mmol/g (dry) on IRA-458(Cl^-).

being directly exposed to the external solution, as compared to spherical particles of commercial resins.

CONCLUSIONS

Textile-grade polyacrylonitrile (PAN) fiber *Cashmilon*™ containing 92% (w/w) acrylonitrile has been chemically coated with polyethylenimine (PEI) resin of molecular weight 60,000 after converting about 15% of the nitrile groups on the fiber into carboxylic acid groups by hydrolysis. The coated PEI is insolubilized by treatment with glutaraldehyde and then quaternized by reaction with ethyl chloroacetate. The resulting sorbent fiber, PAN(QPEI.XG)(Cl^-), containing about 29% (w/w) gel-coated resin, exhibits strong binding to $[Ag(S_2O_3)_2]^{3-}$, attaining saturation sorption even at low concentrations (~4 m*M*) of the sorbate. Whereas $[Ag(S_2O_3)_2]^{3-}$ has higher sorption and stronger binding than $S_2O_3^{2-}$ on the gel-coated sorbent, these two species have only comparable sorptions and binding strengths on the commercial sorbent IRA-458(Cl^-). Consequently, PAN(QPEI.XG)(Cl^-) exhibits much higher selectivity for $[Ag(S_2O_3)_2]^{3-}$ sorption than does IRA-458(Cl^-) in the presence of excess $S_2O_3^{2-}$. In the presence of excess Cl^- ions, the $[Ag(S_2O_3)_2]^{3-}$ sorption capacity of IRA-458(Cl^-) is drastically reduced to less than that of the gel-coated sorbent.

A characteristic feature of the $[Ag(S_2O_3)_2]^{3-}$ sorption behavior of the fibrous sorbent is that nearly 80% of the saturation sorption is reached very fast (in 10 s), followed by an abrupt fall or leveling off trend in the rate of sorption, in sharp contrast to the sorption behavior of the conventional bead-form sorbent which attains only about 12% of equilibrium sorption in 10 s. A similarly striking difference is also observed in the rate of stripping of the sorbed silver complex from the two sorbents with 4*M* HCl (Fig. 13). The sorption of $[Ag(S_2O_3)_2]^{3-}$ in the initial short period on the resin-coated fiber fits to the shell-core model for a cylindrical sorbent with large length/diameter ratio.

The authors thank Dr. P. R. Achar, Deputy Manager R and D, Indian Petrochemicals Corp., Baroda, for supplying polyacrylonitrile fiber used in this work.

References

1. Wase, D. A. J.; Forster, C. F. Biosorbents for Metal Ions; Taylor and Francis: London, 1997.
2. Yiacoumi, S.; Tien, C. Kinetics of Metal Ion Adsorption from Aqueous Solutions: Models, Algorithms and Applications; Kluwer: Dordrecht, 1995.
3. Harris, W. I. Eur. Pat. Appl. 101,943 (Cl. C08F237/02) (1984).
4. Fries, W.; Naples, J. O. Eur. Pat. Appl. 361,685 (Cl. B01539/20) (1990).
5. Chanda, M.; Rempel, G. L. Ind Eng Chem Res 1993, 32, 726.
6. Chanda, M.; Rempel, G. L. Ind Eng Chem Res 1994, 3, 623.
7. Chanda, M.; Rempel, G. L. React Polym 1995, 25, 25.
8. Chanda, M.; Rempel, G. L. Chem Eng Sci 1999, 54, 3723.
9. Chanda, M.; Rempel, G. L. Ind Eng Chem Res 2001, 40, 1624.
10. Chanda, M.; Rempel, G. L. Sep Sci Tech 2001, 36, 3487.
11. Chanda, M.; Rempel, G. L. Ind Eng Chem Res 2003, 42, 5647.
12. Chanda, M.; Sarkar, A.; Chen, Z. J Polym Mater 2004, 21, 21.
13. Finar, I. L. Organic Chemistry, Vol 1: The Fundamental Principles, 6th ed.; Addison Wesley Longman: Harlow, 1973.
14. Nemerow, N. L.; Dasgupta, A. Industrial and Hazardous Waste Treatment; Van Nostrand Reinhold: New York, 1991.
15. Calmon, C.; Gold, H., Eds.; Ion Exchange for Pollution Control; CRC Press: Boca Raton, 1979; Vol. I.
16. Muzzarelli, R. Natural Chelating Polymers; Pergamon: New York, 1973.
17. Lasko, C. L.; Hurst, M. P. Environ Sci Tech 1999, 33, 3622.
18. Vogel, A. I. A Textbook of Quantitative Inorganic Analysis, 3rd ed.; ELBS and Longmans Green: London, 1962.
19. Hill, J. O.; Lim, S. Thermochim Acta 1991, 188, 255.
20. Butler, J. A. V.; Ockrent, C. J Phys Chem 1931, 34, 497.
21. Jain, J. S.; Snoeyink, V. L. J Water Pollut Con F 1973, 45, 2643.
22. LeVan, M. D.; Vermeulen, T. J Phys Chem 1981, 85, 3247.
23. Bhandari, V. M.; Juvekar, V. A.; Patwardhan, S. R. Sep Sci Tech 1992, 27, 1043.